Journal of Geophysical Research: Space Physics

RESEARCH ARTICLE
10.1029/2018JA025951

Observability of Callisto's Inductive Signature During the JUpiter ICy Moons Explorer Mission

Lucas Liuzzo[1], **Sven Simon**[1], **and Moritz Feyerabend**[2]

[1]School of Earth and Atmospheric Sciences, Georgia Institute of Technology, Atlanta, GA, USA, [2]Institute for Theoretical Physics, University of Braunschweig, Braunschweig, Germany

Key Points:
- We present a model of Callisto's magnetic environment during the 12 upcoming flybys of the JUICE spacecraft
- Induction signatures from Callisto's interior will likely be obscured by Alfven wings during several flybys
- Plasma interaction will generate ambiguities in interpretation of JUICE magnetometer observations

Supporting Information:
- Supporting Information S1
- Data Set S1
- Figure S1
- Figure S2
- Figure S3
- Figure S4
- Figure S5
- Figure S6
- Figure S7

Correspondence to:
L. Liuzzo,
lucas.liuzzo@eas.gatech.edu

Citation:
Liuzzo, L., Simon, S., & Feyerabend, M. (2018). Observability of Callisto's inductive signature during the JUpiter ICy moons Explorer mission. *Journal of Geophysical Research: Space Physics*, *123*, 9045–9054. https://doi.org/10.1029/2018JA025951

Received 1 AUG 2018
Accepted 7 OCT 2018
Accepted article online 11 OCT 2018
Published online 8 NOV 2018

Abstract Using hybrid simulations and analytical calculations, we investigate the observable magnetic perturbations during the 12 planned Callisto flybys of the *JUpiter ICy moons Explorer* mission. During four of these encounters, Callisto will be embedded within Jupiter's magnetospheric current sheet. In these cases, Callisto's Alfvén wings and ramside magnetic field pileup will partially obscure any magnetic signatures associated with induction in a conducting layer at the moon, thereby severely complicating attempts to further constrain properties of a possible subsurface ocean. During one of these flybys, the plasma interaction will even generate magnetic signatures that are qualitatively similar to an induced field from the moon's interior. In this case, highly accurate measurements of the upstream flow parameters and Callisto's ionosphere are required to disentangle the induction signal from plasma effects. For the remaining eight encounters, Callisto's plasma interaction is expected to be sufficiently weak for an unobstructed observation of the moon's inductive signature.

Plain Language Summary Jupiter's moon Callisto may possess a salty water ocean beneath its icy surface. Due to time variations of Jupiter's magnetic field near Callisto's orbit, electric currents would be induced in such an ocean, generating magnetic field perturbations detectable outside of the moon. Therefore, magnetometer observations near Callisto can be used to prove the existence and constrain the properties of such a subsurface ocean. However, Callisto is also embedded within Jupiter's magnetosphere and is continuously exposed to a flow of plasma particles that rotate synchronously with the planet. The deflection of this plasma around Callisto generates additional electric currents and associated magnetic perturbations that may obscure the induced field from Callisto's interior. Based on modeling of these plasma currents, we demonstrate that during several flybys of the upcoming JUpiter ICy moons Explorer mission, Callisto's induction signal will be buried by plasma effects beyond recognition. These plasma signatures may even look similar to induced fields and may therefore lead to a false positive identification of the ocean. Our work constrains flyby geometries that are suitable to detect water reservoirs beneath the surfaces of Jupiter's icy moons and is highly relevant for the successful planning of synergistic measurements during the JUpiter ICy moons Explorer mission.

1. Introduction

Driven by the 9.6° tilt of Jupiter's magnetic moment with respect to its rotational axis, the Galilean moons of Jupiter (radius $R_J = 71,492$ km) continually experience a time-varying magnetospheric background field $\mathbf{B}_0$ along their orbits. Of these four moons, Callisto (radius $R_C = 2,410$ km) experiences the largest variability in $|\mathbf{B}_0|$, with values that span more than an order of magnitude at its orbital distance of $26.3R_J$ (from 4 to 40 nT; see, e.g., Kivelson et al., 2004). The orbital periods of the Galilean moons are significantly larger than Jupiter's rotational period, so magnetospheric plasma continually impinges onto their ramside (trailing) hemispheres. The resulting plasma interaction causes the ambient magnetospheric field to pile up at the moons' ramsides, generates a magnetic draping pattern and Alfvén wings, and convects pickup ions from their ionospheres toward downstream (e.g., Neubauer, 1980, 1998).

During the Galileo mission to Jupiter (1995–2003), seven Callisto flybys were performed with the magnetometer active. The first two flybys (C3 and C9) occurred while Callisto was located at large vertical distances to the center of Jupiter's magnetospheric current sheet, where the magnetic perturbations generated by the moon's plasma interaction are weak (e.g., Liuzzo et al., 2015; Zimmer et al., 2000). The dipolar perturbations

observed by Galileo during C3 and C9 were therefore attributed to currents induced within a possible subsurface ocean (e.g., Khurana et al., 1998; Kivelson et al., 1999; Zimmer et al., 2000) or partially within Callisto's highly conductive ionosphere (Hartkorn & Saur, 2017).

The third Galileo flyby (C10) occurred when Callisto was closer to the center of Jupiter's current sheet, where the magnetospheric background field is reduced and the magnetic perturbations associated with the moon's plasma interaction increase. Therefore, a complex nonlinear coupling between electromagnetic induction and the plasma interaction with Callisto's ionosphere and induced dipole was observed (e.g., Neubauer, 1999). Using a hybrid (kinetic ions and fluid electrons) model, Liuzzo et al. (2016) studied C10 magnetometer data and identified Callisto's inductive response within a quasi-dipolar *core region* near the moon's wakeside surface below altitudes of $1R_C$. Only in this narrow region is the induced dipole nearly unobscured by the magnetic perturbations associated with the plasma interaction. During its final four Callisto flybys (C21, C22, C23, and C30), Galileo did not detect any inductive signature due to a combination of unsuitable flyby trajectories and Callisto's proximity to the center of Jupiter's current sheet (Liuzzo et al., 2017).

Nearly 30 years later, another spacecraft will visit Callisto. The *JUpiter ICy moons Explorer* (JUICE; Grasset et al., 2013) mission is scheduled to arrive at Jupiter in late 2029 and, during its approximately 4-year lifetime, is slated to perform 12 targeted Callisto flybys. One major goal for the Callisto flybys is to further constrain the conductivity, thickness, and depth of the possible subsurface ocean by detecting its inductive signature. To constrain these properties, it is imperative that JUICE obtain a more comprehensive picture of Callisto's induced magnetic environment than Galileo. While measurements from three Galileo flybys succeeded in detecting an inductive signature, they were not suitable to rigorously constrain (i) the ocean's properties and (ii) the contribution of Callisto's ionosphere to the observed magnetic perturbations (e.g., Zimmer et al., 2000).

Based on our current understanding of Callisto's plasma environment, this study analyzes the planned Callisto encounters by combining hybrid and analytical modeling to predict the magnetic perturbations JUICE will observe. We identify regions sampled by the 12 planned flybys that are suitable to detect the induced dipole in the complex admixture of induction and plasma interaction. We demonstrate that Callisto's inductive response will likely be obscured by its plasma interaction along the trajectories of at least three planned encounters and that the magnetic perturbations observable during a fourth cannot be unambiguously attributed to induction or plasma interaction alone. Additionally, we show that if the source of Callisto's inductive response has not changed with time, the magnetic perturbations detectable during the first JUICE flyby (8C1) will be nearly identical to those observed during the Galileo C9 encounter.

2. Modeling Callisto's Magnetic Environment During the JUICE Flybys

Displayed in Figure 1 are the 12 Callisto flyby trajectories planned for JUICE, projected onto the $x = 0$, $y = 0$, and $z = 0$ planes of the Cartesian CphiO coordinate system, in which unit vector $\hat{\mathbf{x}}$ is aligned with the corotation direction, $\hat{\mathbf{y}}$ points toward Jupiter, and $\hat{\mathbf{z}}$ completes the right-handed set. Arrows denote the direction of travel for JUICE during each flyby. Specific ephemeris data for each flyby are included in Table 1 and have been obtained via SPICE (Acton, 1996) using the latest kernels for the JUICE mission (CReMA 3.2, available at the mission web page). During just over a year, JUICE will sample different regions of Callisto's magnetic environment at a wide range of closest approach (C/A) altitudes, local times, System III Longitudes, and distances to the center of Jupiter's current sheet (h_{cs}). Of note is the 8C1 flyby, which will occur in the moon's equatorial ($z = 0$) plane and at a local time, h_{cs} value, and along a trajectory *nearly identical* to the Galileo C9 flyby (see also Khurana et al., 1998). After 8C1, the flybys gradually reach more polar latitudes until the 14C6 encounter, as Callisto will be used to increase the inclination of JUICE against the orbital planes of the icy moons to nearly 30° (Grasset et al., 2013). The seventh (15C7) through tenth (18C10) Callisto flybys will aid in returning the spacecraft to an equatorial orbit where the final two flybys of the moon (22C11 and 23C12) will occur.

Various modeling studies of magnetic field observations from the Galileo era suggest that when Callisto is located at distances $|h_{cs}|$ greater than approximately $3.2R_J$, the plasma interaction is weak and does not significantly obscure the induced dipole (e.g., Liuzzo et al., 2015; Zimmer et al., 2000). In such cases, a purely dipolar field explains the observed magnetic signatures very well. Therefore, JUICE flybys that occur at even larger $|h_{cs}|$ values (8C1, 10C2, 12C4, 13C5, 15C7, 16C8, 18C10, and 22C11; see Table 1) can be expected to detect Callisto's unobscured inductive response. However, for flybys that occur with Callisto located at smaller $|h_{cs}|$ values (11C3, 14C6, 17C9, and 23C12), the moon's plasma interaction may partially obscure the induced

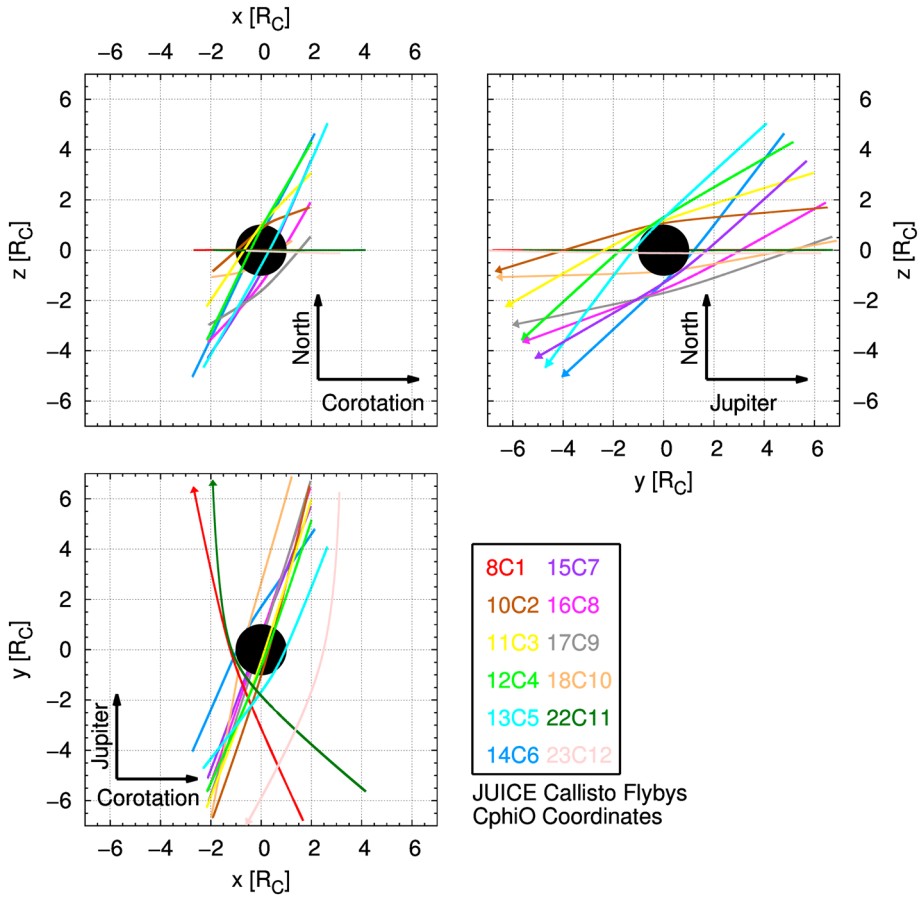

Figure 1. Trajectories of the JUpiter ICy moons Explorer (JUICE) Callisto flybys projected onto the (counterclockwise from top right) $x = 0$, $y = 0$, and $z = 0$ planes of the CphiO coordinate system. Arrows denote the direction of travel.

dipole. Understanding Callisto's magnetic environment during these four flybys is the main goal of our study.

We use the AIKEF hybrid code (Liuzzo et al., 2015, 2016, 2017, 2018) to investigate the magnetospheric interaction with Callisto's ionosphere and induced dipole as expected during the 11C3, 14C6, 17C9, and 23C12 JUICE encounters. Furthermore, we apply the model in a similar way as Liuzzo et al. (2015) to study the JUICE 8C1 flyby (with $|h_{cs}| \approx 4.4R_J$) and to confirm that the plasma interaction is indeed unable to obscure the induced dipole for large $|h_{cs}|$ values. For the remaining seven encounters, an analytical expression for Callisto's induced dipole is sufficient to determine the observable magnetic perturbations along the trajectories, as the plasma interaction is expected to be weak. The expected magnetic signatures for these seven flybys are available in the supporting information.

The AIKEF model treats ions as individual macroparticles, whereas electrons are a massless, charge-neutralizing fluid (Müller et al., 2011). Such a hybrid approach is required for Callisto, since ion gyroradii can be up to 10 times the size of the moon itself (Kivelson et al., 2004), generating large asymmetries in the local plasma flow pattern and associated electromagnetic perturbations (Liuzzo et al., 2015). The model of Callisto's atmosphere used within AIKEF is consistent with observations, and its ionosphere is generated by photoionization and electron impacts. Callisto's induced field is represented by a static dipole moment centered at the moon; see equation (1) in Liuzzo et al. (2016). AIKEF has been applied extensively to investigate Callisto's thermal and energetic plasma environment and has been used to successfully explain magnetic field and plasma measurements from multiple Galileo flybys (Liuzzo et al., 2015, 2016, 2017, 2018). For this study, the model is run with at least 20 macroparticles per cell and operates on a hierarchical grid to achieve a peak spatial resolution of $0.03R_C$. More detailed discussions of the model are given in our aforementioned studies.

In Table 1, the background magnetic field vector $\mathbf{B}_0$ at C/A of each flyby corresponds to Callisto's System III Longitude and is obtained from Figure 1b of Kivelson et al. (1999). Values for the upstream number density

Table 1
The JUICE Flybys of Callisto

Flyby	Date	C/A time (UTC)	$d_{C/A}$ (R_C)	λ_{III} (°)	h_{cs} (R_J)	LT (h)	$\mathbf{B}_0$ (nT)	n_0 (cm^{-3})	M_A	M_{MS}	Dipolar induction signature?
8C1	13 Oct 2030	10:03:06	0.171	9.1	−4.35	05:05	$+5\hat{\mathbf{x}} + 39\hat{\mathbf{y}} - 15\hat{\mathbf{z}}$	0.036	0.159	0.158	Expected
10C2	13 Dec 2030	11:01:09	0.083	349.5	−3.86	20:35	$+5\hat{\mathbf{x}} + 37\hat{\mathbf{y}} - 14\hat{\mathbf{z}}$	0.049	0.195	0.194	Expected
11C3	30 Dec 2030	03:32:11	0.083	117.3	+0.56	20:29	$+2\hat{\mathbf{x}} + 5\hat{\mathbf{y}} - 12\hat{\mathbf{z}}$	0.149	1.033	0.833	Obscured
12C4	15 Jan 2031	19:51:49	0.083	238.2	+3.51	20:23	$-7\hat{\mathbf{x}} - 36\hat{\mathbf{y}} - 15\hat{\mathbf{z}}$	0.059	0.216	0.213	Expected
13C5	1 Feb 2031	12:12:00	0.083	0.0	−4.20	20:17	$+5\hat{\mathbf{x}} + 38\hat{\mathbf{y}} - 15\hat{\mathbf{z}}$	0.040	0.171	0.171	Expected
14C6	25 Apr 2031	22:40:46	0.083	274.3	+1.20	19:50	$-5\hat{\mathbf{x}} - 26\hat{\mathbf{y}} - 14\hat{\mathbf{z}}$	0.137	0.435	0.427	Ambiguous
15C7	12 May 2031	15:00:42	0.083	35.5	−4.32	19:44	$+5\hat{\mathbf{x}} + 39\hat{\mathbf{y}} - 15\hat{\mathbf{z}}$	0.037	0.160	0.159	Expected
16C8	29 May 2031	07:25:31	0.426	159.5	+3.40	19:38	$-4\hat{\mathbf{x}} - 33\hat{\mathbf{y}} - 14\hat{\mathbf{z}}$	0.063	0.245	0.244	Expected
17C9	14 Jun 2031	23:49:51	0.646	283.3	+0.52	19:32	$-4\hat{\mathbf{x}} - 18\hat{\mathbf{y}} - 13\hat{\mathbf{z}}$	0.150	0.604	0.582	Obscured
18C10	1 Jul 2031	15:46:27	0.083	30.7	−4.41	19:25	$+6\hat{\mathbf{x}} + 39\hat{\mathbf{y}} - 16\hat{\mathbf{z}}$	0.034	0.154	0.153	Expected
22C11	27 Sep 2031	04:38:00	0.083	186.3	+4.33	00:46	$-5\hat{\mathbf{x}} - 39\hat{\mathbf{y}} - 15\hat{\mathbf{z}}$	0.036	0.160	0.159	Expected
23C12	25 Nov 2031	10:18:10	1.417	74.2	−2.60	13:44	$+7\hat{\mathbf{x}} + 34\hat{\mathbf{y}} - 15\hat{\mathbf{z}}$	0.091	0.281	0.279	Obscured

Note. Planned spacecraft ephemeris data and expected upstream plasma parameters during the flybys. Closest approach time and altitude ($d_{C/A}$) of each flyby are given, as well as Callisto's System III Longitude (λ_{III}), vertical distance (h_{cs}) above (+) or below (−) the center of Jupiter's magnetospheric current sheet, and local time (LT). The background magnetic field ($\mathbf{B}_0$) and number density (n_0) correlate with λ_{III} and h_{cs}, respectively, and are used to calculate the Alfvénic (M_A) and magnetosonic (M_{MS}) Mach numbers. Observability of a dipolar induction signature is also noted.

n_0 are calculated from $n_0 = \tilde{n}\exp\left(-\left(h_{cs}/H\right)^2\right)$. This equation uses the planned h_{cs} value during the flybys, a base density of $\tilde{n} = 0.153$ cm^{-3}, and a magnetospheric current sheet scale height at Callisto's orbital distance of $H = 3.61R_J$ (Bagenal & Delamere, 2011). An average mass for the upstream ions of 16 amu is used, with a bulk velocity of $\mathbf{u}_0 = u_0\hat{\mathbf{x}} = 192\hat{\mathbf{x}}$ km/s, and an upstream temperature of 650 eV (e.g., Belcher, 1983; Kivelson et al., 2004).

We note that for the 11C3 flyby, these parameters would result in a supermagnetosonic plasma upstream of Callisto, which is theoretically possible when combining measurements from multiple Voyager and Galileo instruments (see Table 21.2 in Kivelson et al., 2004). However, supermagnetosonic upstream conditions have never been measured in situ near the orbit of Callisto nor anywhere else within the Jovian magnetosphere. Therefore, an upstream plasma temperature of 1,550 eV for the 11C3 flyby is used. This value is still within the temperature range observed by Voyager and Galileo at Callisto's orbital distance (Bagenal et al., 2016; Belcher, 1983) and ensures that the upstream plasma conditions are submagnetosonic. As long as the incident flow remains submagnetosonic, the plasma temperature has only minor quantitative impact on the modeled magnetic field signatures near Callisto, as is also consistent with hybrid simulation results of Simon et al. (2007) for Saturn's moon Titan.

For any of the upcoming Callisto flybys, an exact match between the upstream plasma density and velocity values from JUICE and those obtained by, for example, Kivelson et al. (2004) or Bagenal and Delamere (2011), using aggregated Voyager and Galileo data, is not expected. The latter represent an *average state* gleaned from many measurements of the plasma environment near Callisto's orbital distance. However, slight deviations of values observed during a specific flyby from the averaged quantities used in our simulations would mainly affect the Alfvénic Mach number and hence the inclination of the Alfvén characteristics against the background field. This has only minor quantitative influence on the observable magnetic field perturbations near Callisto, especially at C/A altitudes below $1R_C$, where most of the JUICE flybys will occur.

3. Results

Displayed in Figures 2a–2d are the modeled B_x, B_y, and B_z perturbations along the 11C3, 14C6, 17C9, and 23C12 flybys, during which the magnetospheric plasma interaction with Callisto's ionosphere and induced dipole is expected to be strong. The magnetic field of a purely dipolar inductive signature is shown in blue,

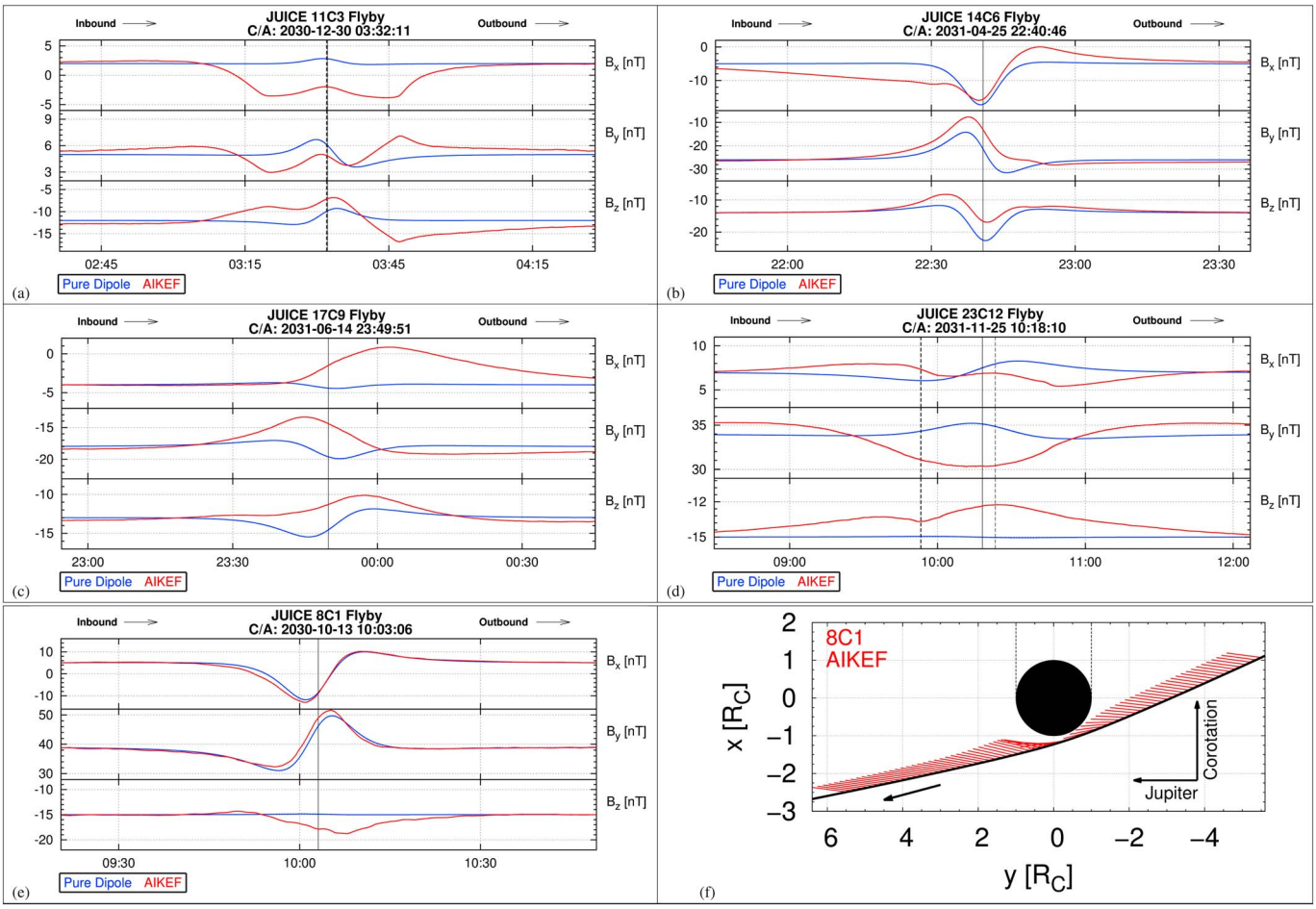

Figure 2. (a–e) Synthetic JUpiter ICy moons Explorer (JUICE) magnetic field time series for select Callisto flybys considering (blue) a purely dipolar induction signature and (red) plasma interaction with Callisto's ionosphere and induced dipole. Vertical black lines denote (solid) C/A of the spacecraft and (dashed) Callisto's geometric plasma shadow, defined by $\sqrt{y^2+z^2} \leq 1R_C$ and $x \geq 1R_C$. (f) Modeled magnetic field vectors projected onto the 8C1 flyby plane, which coincides with the $z = 0$ plane.

whereas the magnetic signatures from the plasma interaction with Callisto's ionosphere and induced dipole calculated by AIKEF are shown in red. Additionally, Figure 2e shows the modeled magnetic field time series for the 8C1 flyby (during which the plasma interaction is expected to be weak), and Figure 2f shows the detectable magnetic field vectors projected onto the flyby plane for this encounter.

The four flybys with strong plasma interaction signatures expected (11C3, 14C6, 17C9, and 23C12 in Figures 2a–2d) all show notable deviations from a pure dipolar signature at Callisto. For the 11C3 and 17C9 flybys (Figures 2a and 2c, respectively), the weak dipolar signature visible in all three components near C/A is almost completely obscured by the plasma interaction. Compared to a pure dipole alone, the plasma-generated B_x and B_y perturbations are even of a different orientation. For the wakeside 23C12 flyby (see Figure 2d), the large C/A altitude of $1.4R_C$ suggests that JUICE will miss the wakeside quasi-dipolar core region where Callisto's induced field would dominate any plasma interaction effects. This situation is similar to the scenario observed by Galileo at Callisto during the C22 flyby (Liuzzo et al., 2017). Figure 2d shows that for 23C12, the B_x and B_y perturbations generated by the plasma interaction (red) are nearly in antiphase with those generated by an induced dipole alone (blue). For these three JUICE flybys, the spacecraft will *not* be able to identify Callisto's inductive response in isolation. Therefore, constraining properties of Callisto's putative subsurface ocean would require precise knowledge of upstream plasma parameters in addition to the structure of Callisto's atmosphere/ionosphere at the time of these flybys. Only then would it be possible to assess the contribution of the induced field to the observed plasma interaction signatures such as, for example, the diameter of the Alfvén wing flux tubes perpendicular to the wing characteristics (Neubauer, 1999). The 14C6 encounter will be the only flyby where the observable perturbations from the plasma interaction are qualita-

tively similar to those of a pure dipole. However, Figure 2b shows that JUICE will pass through regions where the plasma interaction signatures are quantitatively different from those of a dipole.

To understand the cause of the plasma perturbations expected during these four flybys, Figure 3 shows two-dimensional slices through Callisto's magnetically perturbed environment for each encounter. Magnetic field components are shown in the plane containing the point of C/A, the vector $\mathbf{u}_0$, and the expected spacecraft velocity vector, averaged over $\pm$10 s around C/A of each flyby. In these panels, the horizontal axes are parallel to the x axis of CphiO, whereas the vertical axes are parallel to the CphiO $x = 0$ plane and centered around C/A. Because the 23C12 flyby will nearly occur in the $z = 0$ plane, the vertical axis in Figures 3j–3l coincides with the CphiO y axis.

Figures 3a–3c show the magnetic perturbations in the 11C3 flyby plane. This encounter will occur north of Callisto's equatorial plane, and JUICE will travel through the northern (here: Jupiter-averted) Alfvén wing. For a purely southward magnetospheric background field $\mathbf{B}_0$, the Alfvén wing characteristics would be contained within the $y = 0$ plane of the CphiO system (Neubauer, 1980). However, due to the expected orientation of $\mathbf{B}_0$ during 11C3 (see Table 1), the plane containing the characteristics is rotated around the $+x$ axis in a clockwise (right-handed) direction by an angle of approximately 23°. Due to the weak, nonzero $B_{x,0}$ component of the background field, the draping pattern is also slightly asymmetric between both hemispheres (Simon & Motschmann, 2009). Within the northern Alfvén wing, the draped magnetic field possesses a negative B_x component visible in Figure 3a, which almost exclusively generates the B_x signature observable along the trajectory (see Figure 2a). The induced field generates a slight, 1-nT enhancement in B_x only near C/A, within the center of the expected Alfvén wing crossing. This causes the observable W-like signature visible in the B_x component (red line in Figure 2a). However, the weak central spike of this W will likely be embedded within omnipresent magnetospheric fluctuations of a few nanoteslas observed near Callisto's orbital distance (see, e.g., Liuzzo et al., 2017), and therefore undetectable. Signatures observable in the B_y and B_z components mainly result from JUICE crossing the outer edges of the quasi-parabolic, ramside magnetic pileup barrier at the flanks of Callisto's interaction region (red in Figure 3b; blue in Figure 3c), and the associated magnetic depletion downstream of it (blue in Figure 3b; red in Figure 3c).

For the 17C9 encounter, JUICE will move from Callisto's Jupiter-facing ($y > 0$) hemisphere into its Jupiter-averted ($y < 0$) hemisphere. The inclination of the Alfvén wings against the $y = 0$ plane is even stronger than during 11C3: the plane containing the characteristics will be tilted against the $y = 0$ plane by an angle of approximately 54°. During 17C9, JUICE will travel through the southern (here: Jupiter-averted) Alfvén wing just after C/A. This is indicated by the broad B_x enhancement in Figure 3g and the associated reduction of $|B_y|$ in Figure 3h—perturbations that are again much stronger than those associated with a purely dipolar field. Due to the negative $B_{x,0}$ component of the magnetospheric background field, the wakeside magnetic depletion region is tilted southward out of the moon's equatorial plane by approximately 17° (Simon & Motschmann, 2009) and therefore intersects the flyby plane of the 17C9 encounter. JUICE will intersect this region just before C/A, as visible in B_y and B_z (shaded red in Figures 3h and 3i, respectively). This depletion overcompensates the tendency of the dipole to enhance the magnitude of these components around C/A (see Figure 2c). Any slight changes of n_0 or u_0 would only alter the magnitude of the observable field perturbations, but not their general structure.

For the 23C12 flyby, the Alfvén wing characteristics will be tilted by an angle of approximately 66° against the $y = 0$ plane. Figure 3j shows that the familiar *shamrock leaves* of the induced dipole dominate the B_x perturbations near Callisto's surface. In the flyby plane, which also contains the induced magnetic moment, B_y is reduced near Callisto's *magnetic poles* due to the superposition of the dipole with the magnetospheric background field (see Figure 3k and Liuzzo et al., 2017). However, as demonstrated in Figure 2d, these dipole-dominated regions will *not* be detectable by JUICE. Only without the plasma interaction would the inductive response clearly reach the JUICE trajectory (blue lines in Figure 2d). Rather, the Alfvén wings will partially enclose the two wakeside dipolar shamrock leaves visible in the B_x component, thereby slightly compressing them and preventing the trajectory from intersecting the wakeside quasi-dipolar core region (see Figure 3j). A similar effect contributed to the nondetection of Callisto's induced field during the Galileo C21 flyby; see Figure 3a of Liuzzo et al. (2017). The observable perturbations during 23C12 instead correspond to the southern (here: Jupiter-facing, $y > 0$) and northern (Jupiter-averted, $y < 0$) Alfvén wings with (red) $B_x > 0$ and (blue) $B_x < 0$ in Figure 3j. Additionally, Figure 3j shows that the strength of the B_x perturbations decreases with increasing distance to Callisto. Slight deviations of the Alfvénic Mach number from the value used here

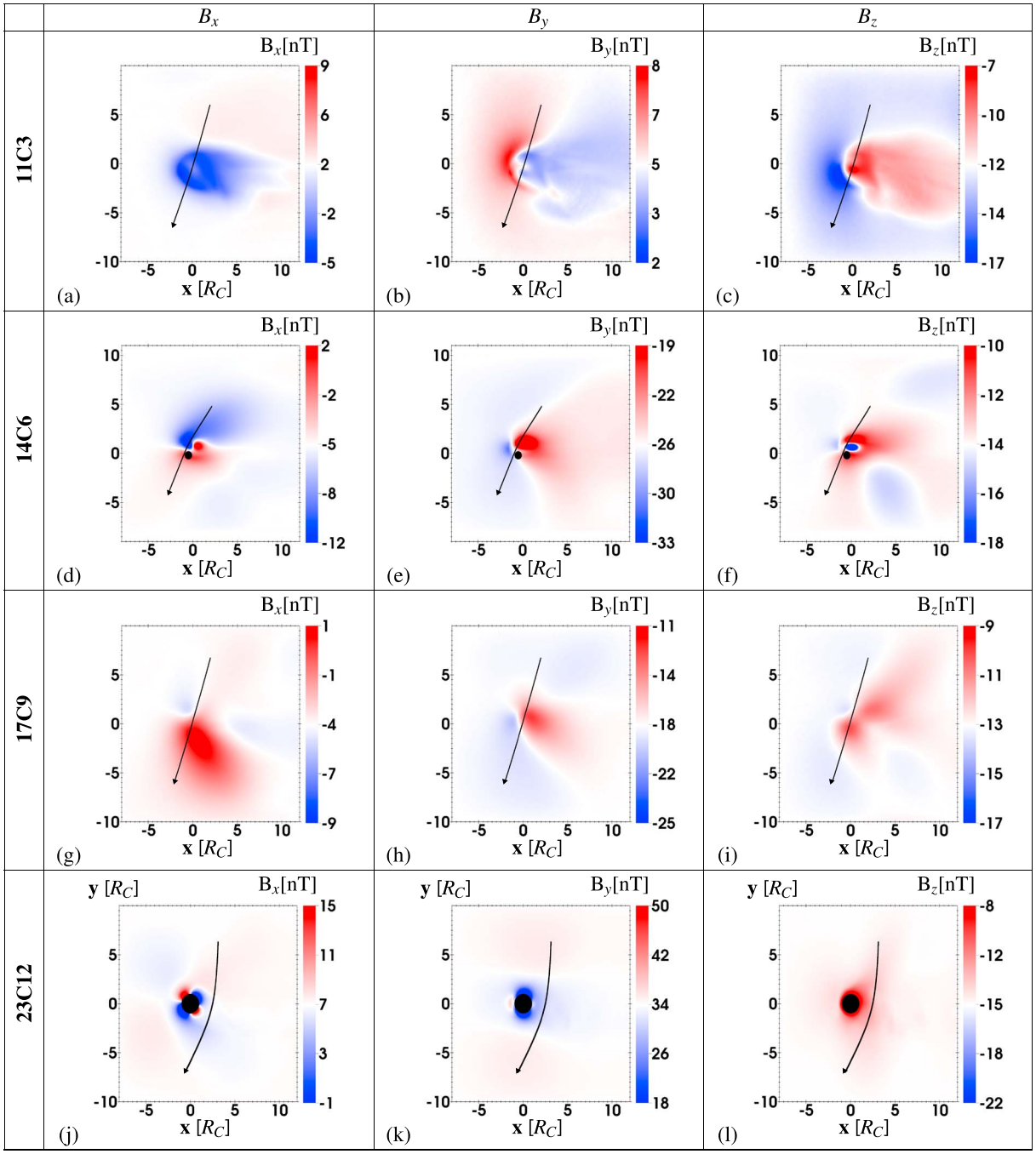

Figure 3. Magnetic field (a,d,g,j) B_x, (b, e, h, k) B_y, and (c, f, i, l) B_z perturbations during select flybys in the plane containing the point of C/A, upstream bulk velocity vector $\mathbf{u}_0$, and the spacecraft velocity vector, averaged ±10 s around C/A of the respective flyby (see Figure 1). Regions where Callisto intersects each plane are represented by a black circle, where applicable.

(see Table 1) would change the distance to Callisto at which the draped field lines are intersected by JUICE and thus affect only the strength of the observable B_x perturbations. The JUICE trajectory also intersects the wakeside magnetic depletion region in B_y (see Figure 3k), and Figure 3l illustrates that the B_z perturbations along the trajectory stem *exclusively* from the plasma interaction. Because the induced magnetic moment and the JUICE trajectory are both contained within the $z = 0$ plane, there are no B_z perturbations generated by the dipole alone along the trajectory. In summary, if the 23C12 trajectory were located closer to Callisto's wakeside surface, the spacecraft could detect the induced dipole field within the wakeside quasi-dipolar core region, despite the strong plasma interaction.

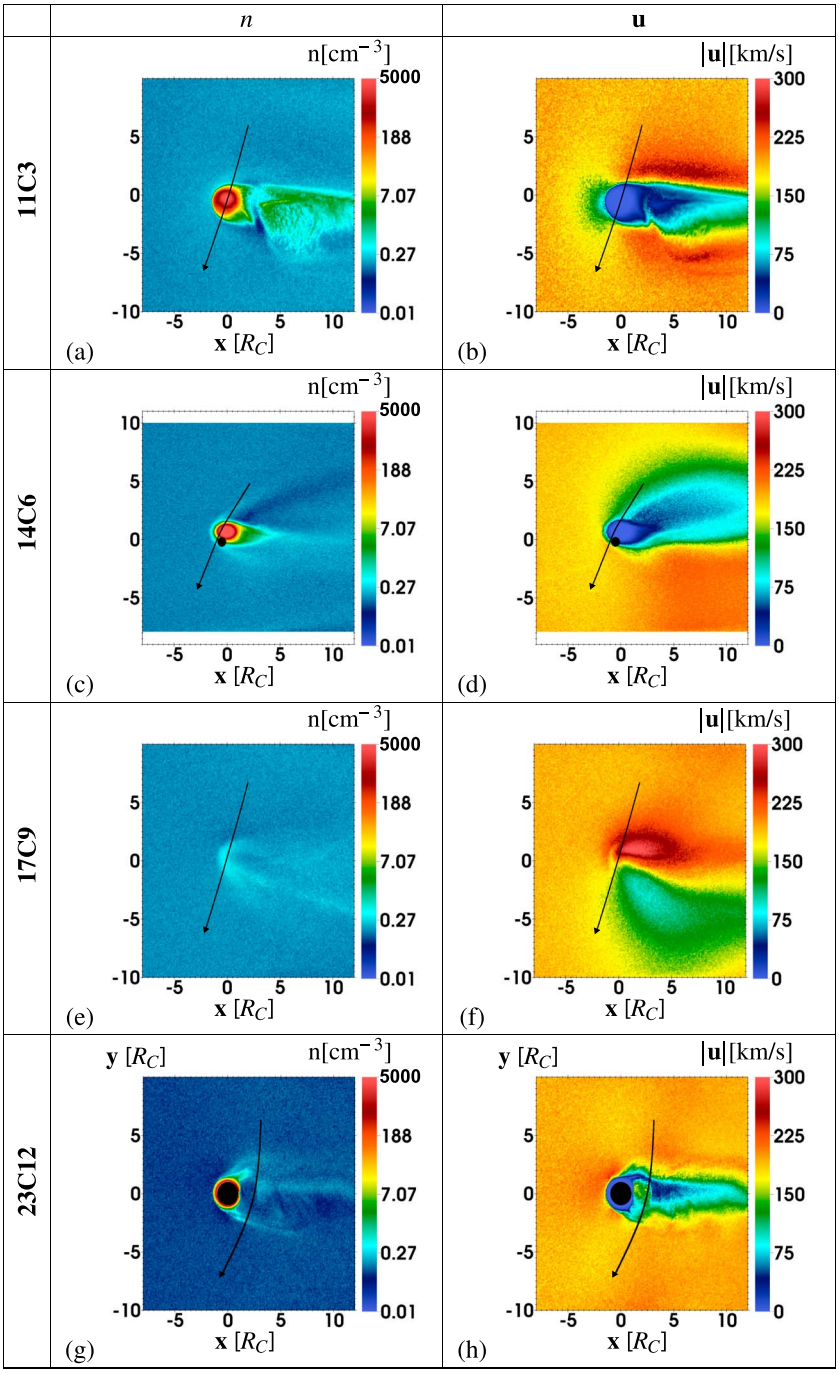

Figure 4. (a, c, e, and g) Total electron density and (b, d, f, and h) bulk velocity in the flyby planes of the 11C3, 14C6, 17C9, and 23C12 JUICE encounters of Callisto. The layout is similar to Figure 3.

The only flyby of these four where Callisto's induced field is not completely obscured by the plasma interaction is 14C6 (see Figure 2b). Still, Figures 3d–3f show that the observable features cannot be unambiguously attributed to a pure dipole. For this flyby, the inclination of the plane containing the Alfvén wing characteristics is tilted by approximately 62° against the $y = 0$ plane, and the flyby trajectory is almost completely contained within the wing plane. Signatures in all three components of the modeled magnetic field are qualitatively similar to dipolar perturbations (see Figure 2b). However, the Alfvén wings generate an offset in magnitude of the perturbations for all three components that, near C/A, is weak in B_x but much stronger in B_y and B_z. Therefore, while the observable magnetic signatures may *look* similar to a purely dipolar field, they are entangled with

nonnegligible contributions from plasma currents. The perturbations associated with the Alfvén wings along the 14C6 trajectory have the *same* orientation as those generated by a pure dipole. Even if the induced dipole were absent and the magnetospheric plasma interacted with Callisto's ionosphere alone, the orientation of the perturbations within the Alfvén wings along 14C6 would still be qualitatively similar to those shown in Figure 2b; see also Liuzzo et al. (2015). Thus, for 14C6, the plasma interaction with the ionosphere may in principle lead to a false positive detection of an induction signal. The influence of the plasma interaction can only be corrected for if the exact parameters of the upstream plasma, as well as the density profile of Callisto's ionosphere, can be thoroughly constrained through JUICE data. Otherwise, this flyby will not be suitable to further constrain, for example, the slight uncertainties in the strength of Callisto's induced magnetic moment found by Zimmer et al. (2000).

Figures 2e and 2f show the expected magnetic field perturbations along the 8C1 trajectory. Again, the magnetic field generated by Callisto's induced dipole alone is shown in blue (in Figure 2e), while the perturbations from the plasma interaction are shown in red (in Figures 2e and 2f). Similar to the Galileo C9 flyby, 8C1 is a ramside encounter in Callisto's equatorial plane; therefore, the induced field is only observable in B_x and B_y (see Figure 2e). Another similarity between these encounters is the large distance of Callisto from the center of Jupiter's magnetospheric current sheet (see Table 1); thus, during 8C1, Callisto's inductive response is expected to be nearly unobscured by plasma currents. Indeed, Figure 2e shows that the plasma interaction (red) only weakly compresses the induced dipole, causing a slight enhancement in B_x and B_y of less than 2 nT above the pure inductive response (blue). Figure 2f shows that these dipolar perturbations are observable along the trajectory over a length of approximately $3R_C$, with an orientation similar to that observed during the Galileo C9 flyby (see Figure 3b in Khurana et al., 1998). The only noticeable plasma interaction signature occurs in B_z due to pileup at Callisto's ramside (see Figure 2e), as the induced dipole makes no contribution to this component along the equatorial trajectory. Thus, due to the combination of a suitable flyby trajectory with weak plasma interaction currents, magnetometer observations from 8C1 can easily be applied to further constrain properties of Callisto's putative subsurface ocean.

For the sake of completeness, Figure 4 shows the (left column) total electron number density n and (right column) magnitude of the bulk velocity $\mathbf{u}$ in the flyby planes of the 11C3, 14C6, 17C9, and 23C12 encounters. Only the 11C3 and 14C6 encounters display strong density enhancements by several orders of magnitude above background near C/A along their respective flyby trajectory. These observable enhancements should look qualitatively similar to the localized density increase observed by Galileo during the C10 flyby (see Gurnett et al., 2000; Liuzzo et al., 2016). For the 17C9 and 23C12 flybys, Figure 4 illustrates that regions of strong ionospheric outflow will likely *not* be intersected during these encounters, mainly due to the orientation of the background magnetic field. For each of these four flybys, Callisto's plasma interaction generates a distinct velocity deflection pattern, with regions of alternating enhanced and decreased velocity in each flyby plane. Thus, Callisto's plasma interaction and wake should leave a clear imprint in velocity observations, should they become available during these four encounters.

4. Conclusions

We have analyzed the 12 planned JUICE flybys of Callisto to understand the magnetic field perturbations that may be observable along their trajectories. During four of the planned encounters (11C3, 14C6, 17C9, and 23C12), Callisto will be located close to the center of Jupiter's magnetospheric current sheet. Therefore, Callisto's inductive response will be *buried* within the magnetic perturbations generated by the plasma interaction with Callisto's ionosphere and induced dipole.

The remaining eight flybys, including 8C1, occur far from the center of Jupiter's magnetospheric current sheet where the plasma interaction is expected to be weak. In our study, the observable magnetic perturbations during these encounters correspond to induction within a spherically symmetric conducting layer beneath Callisto's surface (e.g., Seufert et al., 2011; Zimmer et al., 2000). The induced dipolar response of such a layer is able to explain magnetometer data from all Galileo flybys where Callisto's induced field was observed (C3, C9, and C10; e.g., Khurana et al., 1998; Kivelson et al., 1999; Liuzzo et al., 2016). Induction within Callisto's nonspherical ionosphere is not included in this representation. This effect would also generate higher-order terms in the induced field (Hartkorn & Saur, 2017), which may be observable at low altitudes where some of the remaining eight JUICE flybys will occur. Therefore, deviations between our modeled results (as provided in Figures 2e and 2f and the supporting information) and JUICE observations for these eight flybys can be

used to identify a possible contribution of induction within Callisto's ionosphere to the observed magnetic perturbations. Nonetheless, in order to constrain this subtle effect, detailed measurements characterizing the structure and composition of Callisto's ionosphere must be obtained at the time of each of these upcoming JUICE encounters.

Acknowledgments
Authors L. L. and S. S. are supported through the National Aeronautic and Space Administration *Solar Systems Working 2014* program, grant NNX15AL52G. L. L. thanks Olivier Witasse for helpful discussions on the specifics of the JUICE mission. All simulations were carried out on the ATLAS Cluster at the Georgia Institute of Technology. The latest SPICE kernels for the JUICE mission at the time this publication (CReMA 3.2) were used for this study and can be downloaded at *https://www.cosmos.esa.int/web/spice/spice-for-juice*. Results from the AIKEF hybrid model and figures presented in this publication can be downloaded at *https://github.com/lukeliuzzo/JUICE* or shared following requests to the corresponding author.

References

Acton, C. (1996). Ancillary data services of NASA's navigation and ancillary information facility. *Planetary and Space Science*, *44*(1), 65–70.

Bagenal, F., & Delamere, P. A. (2011). Flow of mass and energy in the magnetospheres of Jupiter and Saturn. *Journal of Geophysical Research*, *116*, A05209. https://doi.org/10.1029/2010JA016294

Bagenal, F., Wilson, R. J., Siler, S., Paterson, W. R., & Kurth, W. S. (2016). Survey of Galileo plasma observations in Jupiter's plasma sheet. *Journal of Geophysical Research: Planets*, *121*, 871–894. https://doi.org/10.1002/2016JE005009

Belcher, J. W. (1983). The low-energy plasma in the Jovian magnetosphere. *Physics of the Jovian magnetosphere*, *1*, 68–105.

Grasset, O., Dougherty, M., Coustenis, A., Bunce, E., Erd, C., Titov, D., et al. (2013). JUpiter ICy moons Explorer (JUICE): An ESA mission to orbit Ganymede and to characterise the Jupiter system. *Planetary and Space Science*, *78*, 1–21. https://doi.org/10.1016/j.pss.2012.12.002

Gurnett, D. A., Persoon, A. M., Kurth, W. S., Roux, A., & Bolton, S. J. (2000). Plasma densities in the vicinity of Callisto from Galileo plasma wave observations. *Geophysical Research Letters*, *27*(13), 1867–1870. https://doi.org/10.1029/2000GL003751

Hartkorn, O., & Saur, J. (2017). Induction signals from Callisto's ionosphere and their implications on a possible subsurface ocean. *Journal of Geophysical Research: Space Physics*, *122*, 11,677–11,697. https://doi.org/10.1002/2017JA024269

Khurana, K. K., Kivelson, M. G., Stevenson, D. J., Schubert, G., Russell, C. T., Walker, R. J., & Polanskey, C. (1998). Induced magnetic fields as evidence for subsurface oceans in Europa and Callisto. *Nature*, *395*(6704), 777–780. https://doi.org/10.1038/27394

Kivelson, M. G., Bagenal, F., Kurth, W. S., Neubauer, F. M., Paranicas, C., & Saur, J. (2004). Magnetospheric interactions with satellites. In F. Bagenal, T. E. Dowling, & W. B. McKinnon (Eds.), *Jupiter: The planet, satellites and magnetosphere* (pp. 513–536). Cambridge, UK: Cambridge University Press.

Kivelson, M. G., Khurana, K. K., Stevenson, D. J., Bennett, L., Joy, S., Russell, C. T., et al. (1999). Europa and Callisto: Induced or intrinsic fields in a periodically varying plasma environment. *Journal of Geophysical Research*, *104*(A3), 4609–4626. https://doi.org/10.1029/1998JA900095

Liuzzo, L., Feyerabend, M., Simon, S., & Motschmann, U. (2015). The impact of Callisto's atmosphere on its plasma interaction with the Jovian magnetosphere. *Journal of Geophysical Research: Space Physics*, *120*, 9401–9427. https://doi.org/10.1002/2015JA021792

Liuzzo, L., Simon, S., Feyerabend, M., & Motschmann, U. (2016). Disentangling plasma interaction and induction signatures at Callisto: The Galileo C10 flyby. *Journal of Geophysical Research: Space Physics*, *121*, 8677–8694. https://doi.org/10.1002/2016JA023236

Liuzzo, L., Simon, S., Feyerabend, M., & Motschmann, U. (2017). Magnetic signatures of plasma interaction and induction at Callisto: The Galileo C21, C22, C23, and C30 flybys. *Journal of Geophysical Research: Space Physics*, *122*, 7364–7386. https://doi.org/10.1002/2017JA024303

Liuzzo, L., Simon, S., & Regoli, L. (2018). Energetic ion dynamics near Callisto. *Planetary and Space Science*. https://doi.org/10.1016/j.pss.2018.07.014, in press.

Müller, J., Simon, S., Motschmann, U., Schüle, J., Glassmeier, K., & Pringle, G. J. (2011). A.I.K.E.F.: Adaptive hybrid model for space plasma simulations. *Computer Physics Communications*, *182*(4), 946–966. https://doi.org/10.1016/j.cpc.2010.12.033

Neubauer, F. M. (1980). Nonlinear standing Alfvén wave current system at Io: Theory. *Journal of Geophysical Research*, *85*, 1171–1178. https://doi.org/10.1029/JA085iA03p01171

Neubauer, F. M. (1998). The sub-Alfvénic interaction of the Galilean satellites with the Jovian magnetosphere. *Journal of Geophysical Research*, *103*, 19,843–19,866. https://doi.org/10.1029/97JE03370

Neubauer, F. M. (1999). Alfvén wings and electromagnetic induction in the interiors: Europa and Callisto. *Journal of Geophysical Research*, *104*, 28,671–28,684. https://doi.org/10.1029/1999JA900217

Seufert, M., Saur, J., & Neubauer, F. M. (2011). Multi-frequency electromagnetic sounding of the Galilean moons. *Icarus*, *214*(2), 477–494. https://doi.org/10.1016/j.icarus.2011.03.017

Simon, S., Boesswetter, A., Bagdonat, T., Motschmann, U., & Schuele, J. (2007). Three-dimensional multispecies hybrid simulation of Titan's highly variable plasma environment. *Annales de Geophysique*, *25*(1), 117–144.

Simon, S., & Motschmann, U. (2009). Titan's induced magnetosphere under non-ideal upstream conditions: 3D multi-species hybrid simulations. *Planetary and Space Science*, *57*(14–15), 2001–2015. https://doi.org/10.1016/j.pss.2009.08.010

Zimmer, C., Khurana, K. K., & Kivelson, M. G. (2000). Subsurface oceans on Europa and Callisto: Constraints from Galileo magnetometer observations. *Icarus*, *147*(2), 329–347. https://doi.org/10.1006/icar.2000.6456